Journal of Advanced Biomedical and Pharmaceutical Sciences

Journal Homepage: http://jabps.journals.ekb.eg

Development and characterization of nanostructure lipid carrier for anti-hepatitis-C virus drug

Omnia E. A. Mahmoud[1], Dina Fathalla[2] , Mahmoud El-Badry[2,3] * and Gamal A. EL-Gendy[2]

[1]Department of Pharmaceutics, Faculty of Pharmacy, Sohag University, Sohag, Egypt
[2]Department of Pharmaceutics, Faculty of Pharmacy, Assiut University, Assiut 71515, Egypt
[3]Assiut International Center of Nanomedicine, Alrajhy Liver Hospital, Assiut University, Assiut 71526, Egypt

Received: September 6, 2023; revised: October 23, 2023; accepted: November 1, 2023

Abstract

Velpatasvir (VLP) as, a medication used to treat hepatitis-C virus (HCV). It has avery low oral bioavailability (25%). The aim of the current work is to prepare VLP loaded nanostructured lipid carriers (VLP- NLCs) as a potential way to enhance VLP aqueous solubility and bioavailability and increase its efficacy. The preparation of VLP-NLCs was carried out using the emulsification - solvent evaporation method, followed by ultrasonication. The prepared nanocarrier was examined for its particle size, zeta potential, entrapment efficiency and in-vitro drug release of the selected formula. VLP-NLCs displayed narrow size distribution, spherical morphologies that were nanosized (105 ± 2.3 nm), and significant drug entrapment efficiencies (> 80%). Particle size ranged between 105 ± 2.3 to 1399 ± 2.8 nm and zeta potential between -14.6 ± 0.2 to -46.0 ± 1.1 mV. High entrapping efficiency was obtained due toincorporation of liquid lipid. The In Vitro release showed prolonged time dependent release. NLC 6 had the best results among the eight prepared formulae. These findings show that NLC is a potential carrier to improve the solubility of drug and enhance its bioavailability.

Keywords
Velpatasvir (VLP); nanostructured lipid carriers (NLCs); particle size; in-vitro drug release

Introduction

Poor solubility, oral bioavailability, and delivery impact about 40% of medications in development and 70% of synthesized medicinal compounds (1, 2). Given a small concentration gradient between the gut and blood arteries, oral administration of drugs with poor solubility results in restricted transport. Similar to parenteral administration, micro suspensions cannot generate acceptable drug levels in body fluids due to low solute concentrations at the injection site (3).

To elevate the saturation solubility of poorly soluble pharmaceuticals in body fluids, new delivery systems have been designed (4). One strategy is to load these medications onto solid lipids serving as nanocarriers in order to boost their solubility (5, 6). The efficiency relies on the ability of these drug-loaded nanoparticles to cross multiple anatomical barriers, to exhibit sustained-release properties, and to be stable at a nanoscale size (3, 7). Numerous types of nanocarriers, among which are solid lipid nanoparticles (SLN), nanostructured lipid carriers (NLC), and lipid- drug conjugates, have been created for this purpose (8, 9).

Lipid nanoparticles create a carrier system with a variety of advantageous properties, such as low toxicity and biodegradable particulate material matrix, harmless degradation products, a high capacity to integrate hydrophilic and lipophilic medicines, regulated release of the incorporated drug, and simple scale- up at a reasonable price (10). NLC, a second-generation of SLN that is brand-new, possesses all SLN qualities and shows significant promise as a site-specific and controlled drug delivery system that outperforms SLN (11, 12).

Greater flexibility in drug loading and drug-hol ding, which is crucial to long-term stability and control of drug release, is one of the distinguishing features of NLC over SLN (13, 14). In nanostructured Liquid carriers NLCs, lipids (i.e., oils) are thoroughly blended and incorporated into a solid lipid matrix to develop lipid carriers, which enable the total lipid content to be raised to as much as 95% (15, 16).

HCV is a common disease as WHO published that 71 million people living with chronic HCV infection worldwide, an escalating liver disease burden resulting in approximately 400,000 deaths per year from liver failure and liver cancer 17), a minority (possibly only 20%) of people with chronic HCV diagnosed (17) and an estimated 1.75 million people newly infected with HCV each year (17) demonstrate the enormous task ahead. The development of direct-acting antiviral (DAA) therapy for chronic HCV infection is one of the great advances in clinical medicine in the past few decades (18).

Efforts to treat HCV have historically been hampered by suboptimal and inadequate treatments. However, the development of direct-acting antivirals (DAAs) has dramatically improved the prospects for HCV treatment and has altered the standard of care.

DAAs block viral production by directly inhibiting one or more steps of the HCV replication cycle. DAAs can be divided into

**** Correspondence:*** *Mahmoud El-Badry*
Tel.: *882141269*
Email Address: *elbadry@aun.edu.eg*

categories – notably NS3/NS4A serine protease inhibitors, NS5A complex inhibitors and NS5B RNA polymerase inhibitors (both nucleoside and non-nucleoside) (19).

These DAAs generate cure rates that approach or exceed 90%. Some combination regimens may have pan genotypic efficacy, which would simplify treatment and monitoring. In this context, velpatasvir VLP is one of the compounds of interest. VLP chemical structure was illustrated in (Fig 1) (20).

VLP is classified as a class IV biopharmaceutical medicine by the Biopharmaceutical Classification System (BCS), with low water solubility and low permeability. At pH 1.2, it is soluble (36 mg/ mL), slightly soluble at pH 2 (3.6 mg/mL), and virtually insoluble at pH > 5 (0.1 mg/mL) (21, 22). The drug's low bioavailability is an outcome of this tendency, since it has been noted that the stomach's pH ranges from 1.3 to 2.5 when one is fasting and rises to 4.5 to 5.8 an hour after eating (23). Likewise, the intragastric pH can instantly increase to >4 even with just a glass of water (24). thereby, it makes sense to establish effective approaches that boost the solubility and bioavailability of VLP

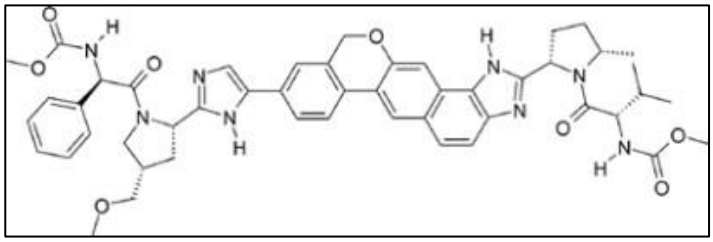

Figure 1. Chemical structure of VLP

Methods and materials

Materials

VLP was generously donated by (Mina pharm Pharmaceuticals (Cairo, Egypt). Stearic acid and liquid paraffin were purchased from El-Nasr Chemicals Co. (Abu Zaabal, Egypt). Tween 80 and oleic acid was purchased from Alpha Chemicals (Cairo, Egypt). Precirol ATO5 (Glycerol distearate) was generously provided as a free sample by Gattefosse Company, France. Other chemicals and reagents were of analytical grades.

Methods

1-Preparation of VLP NLC

VLP-NLCs formulae were prepared by emulsification-ultrasonication method as described in previous researches with some modifications (25, 26). In a nutshell, VLP was dissolved in an amber glass vial of the oily phase made up of stearic acid or Precirol ATO5 and either oleic acid or liquid paraffin dissolved in 1ml chloroform. The vial's oily phase was heated to a temperature of 80 °C, which is higher than the solid lipid melting point. In a tiny beaker, a predetermined amount of water was used to dissolve the surfactant (Tween 80). The aqueous phase was then heated to the same temperature as the oily phase. The hydrophilic surfactant-containing aqueous phase was mixed with the oily component and homogenized under stirring at 1200 rpm and 80°C for 10 minutes. This yielded a coarse emulsion, which was then sonicated using a probe-type sonicator for 10 minutes at 40% of the maximum output to create VLP- NLCs with the appropriate size. Nanoparticles were sonicated and then cooled for two hours at room temperature using magnetic stirrer and allowed to undergo lipid phase crystallization for formation of VLP-NLCs (Fig. 2). The composition of the eight nanoparticles formulae produced is listed in table 1

Figure 2. Appearance of VLP-NLCs

Table 1. Composition of the eight prepared VLP-NLCs.

Formula	*Solid lipid*	*Liquid lipid*	*Solid lipid/ liquid lipid*	*Surfactant*
1	Stearic acid	Oleic acid	70:30	Tween 80 1%
2	Stearic acid	Liquid Paraffin	70:30	Tween 80 1%
3	Precirol ATO5	Oleic acid	70:30	Tween 80 1%
4	Precirol ATO5	Liquid Paraffin	70:30	Tween 80 1%
5	Stearic acid	Oleic acid	30:70	Tween 80 1%
6	Precirol ATO5	Oleic acid	30:70	Tween 80 1%
7	Precirol ATO5	Oleic acid	30:70	Tween 80 1.5%
8	Precirol ATO5	Oleic acid	30:70	Tween 80 2%

II. Characterization of Lipid Nanoparticles

1- Particle Size Analysis

It is a method to determine the particles' mean diameter and the index of polydispersity (PDI) which is a measure of the uniformity of size distribution. Particle size analysis of VLP-NLCs was performed by dynamic light scattering (DLS) using a photon correlation spectrometer Nano ZS (Malvern Instruments, Worcestershire, UK) at 173 °C. Standard operating procedures were used to regulate all settings and analysis outcomes of measurements. All samples were diluted ten times with double distilled water prior to measurements. All the measurements were performed at 25 °C in triplicates (27).

2-Measurement of the surface charge of VLP-NLCs

The electrical charge on the nanoparticles' surfaces is evidence of the colloidal system's physical stability (28). The surface charge of the prepared VLP-NLCs was measured using zeta potential by determining the electrophoretic mobility using the Nano ZS (Malvern Instruments, Worcestershire, UK). All samples were diluted ten times with double distilled water prior to measurements. All the measurements were performed at 25 °C in triplicates.

3-Determination of EE% of VLP in NLC formulae

NLCs containing VLP were separated from the free drug via dialysis. The drug content was assessed spectrophotometrically at 302 nm using UV-visible spectrophotometer (Shimadzu Seisakusho, Ltd., Kyoto, Japan). VLP EE was calculated from the following equation:

$$EE\% = \frac{Z - Y}{Z} \times 100$$

Z and Y are the weight of VLP added in the system and analyzed weight of VLP insupernatant, respectively (29). All procedures are repeated three times and the mean

± SD of EE was calculated

4-Differential Scanning Calorimetry Analysis

Differential Scanning Calorimetry (DSC) analysis was done to study the physical state and polymorphism of the selected NLC 6. The measurements were performed using differential scanning calorimeter, (DSC60; Shimadzu Corporation, Tokyo, Japan). Samples weighing 2-5 mg were heated and scanned between 25° C and 250° C and a heating rate of 10° C/min under nitrogen gas flow (50 ml/min) (30).N_2 was used as purging gas at a rate of 50 mL/min. An empty sealed aluminum pan was used as a reference. DSC analyses were performed on the bulk solid lipid Precirol ATO5, the pure drug (VLP), physical mixture (1:1).

5-Transmission electron microscopy examination (TEM)

The morphology of the VLP-NLCs particles was evaluated by Transmission Electron Microscopy (TEM) model (JEM 100 CX11, Japan). The measurements were done by negative-staining method (31). In simple terms, one drop of the nanoparticle dispersion was applied to the copper grid layer, and any extra droplets were wiped away with filter paper. Following negative staining and room-temperature air drying of the samples, they were ready for the TEM investigation which was done at 15 kV.

6-Wide angle X-ray diffraction (XRD)

The geometric scattering of radiation from crystal planes within nanoparticle dispersion can be determined by wide-angle X-ray diffraction to assess the degreeof crystallinity. X-ray diffractometer model PW 1710 (Philips, Amsterdam, Netherlands), equipped with a copper anode (γ = 1.5406 Å) for radiation was usedto detect the crystallinity of the drug, Precirol A T O 5 and their 1:1 physical mixture. Powdered samples about 10 mm in length were placed on the top of X-ray plates, exposed to a voltage of 40 kV and a 30mA current at room temperature, Samples were scanned from 2θ = 5° to 2θ = 50° with a step of 0.06°/min (32).

7-Fourier transform-infrared spectroscopy (FT-IR)

The FT-IR spectra of the selected NLC 6, corresponding physical mixture and the individual solid components were recorded using FTIR spectrophotometer (IR-470; Shimadzu, Kyoto, Japan). Samples were mixed with KBR (spectroscopic grade) and compressed into disks using hydraulic press before scanning from 4,000 to 500 cm^{-1}.

8-In Vitro Release of VLP

In-vitro dissolution was used to investigate release profile of the selected VLP loaded NLC. Conditions were maintained as described in food and drug administration (FDA) i.e., 75 ± 1 rpm and 37 ˚C. NLC 6 equivalents to 50 mg VLP was exposed to two different dissolution media with pH 1.2 (h y d r o c h l o r i c a c i d) and (P h o s p h a t e b u f f e r) p H 6.8 in water bath shaker for 24 hrs. At predetermined time intervals, samples were withdrawn from dissolution medium and same volume was replaced. Concentration of VLP was calculated from previously constructed calibration curve (33).

Results and discussion

I-Preparation of VLP-NLCs

All VLP- NLCs were prepared successfully using the homogenization ultra- sonication technique. Oleic acid and liquid paraffin were used as liquid lipids. There was neither physical separation nor chemical incompatibility between liquidoils used and all other constituents used in the formulation.

II-Characterization of the prepared VLP-NLC nanoparticles

1- Particle size analysis

The produced VLP-NLCs had particle diameters that varied from 105 ± 2.3 to 1399
± 2.8 nm, which corresponded to the values for the different formulas. For the formulas NLC6 and NLC4, the values of the polydispersity index ranged from 0.33 ± 0.02 0.01 and 0.35 ± 0.07, respectively. From the data showed in Table 2, it is clear that using of oleic acid with Precirol resulted in a reduction in particle size. The superior polydispersity index range, according to the literature, is ≤ 0.5, meaning that six of the eight formulae had excellent particle size distribution while the other two had somewhat wide particle size ranges. To reduce the range of

Table 2. Particle size (Pz), polydispersity index (PDI) and zeta potential of the prepared VLP-NLCs.

Formula	*Solidlipid*	*Liquidlipid*	*Solid lipid/ liquidlipid*	*Surfactant*	*Particle size*	*PDI*	*Zeta potential*
1	Stearicacid	Oleicacid	70:30	Tween 80 1%	669 ± 6.7	0.32 ± 0.07	-21.5 ± 2.0
2	Stearicacid	Liquid Paraffin	70:30	Tween 80 1%	494.5 ± 4.1	0.29 ± 0.01	-30.2 ± 1.6
3	PrecirolATO5	Oleicacid	70:30	Tween 80 1%	157 ± 5.6	0.23 ± 0.01	-28.9 ± 1.6
4	PrecirolATO5	Liquid Paraffin	70:30	Tween 80 1%	1399 ± 2.8	0.35 ± 0.07	-46.0 ± 1.1
5	Stearicacid	Oleicacid	30:70	Tween 80 1%	189.2± 3.1	0.41 ± 0.01	-18.6 ± 0.4
6	PrecirolATO5	Oleicacid	30:70	Tween 80 1%	105 ± 2.3	0.33 ± 0.02	-26.0 ± 0.8
7	PrecirolATO5	Oleicacid	30:70	Tween 80 1.5%	165 ±37.88	0.559 ± 0.03	-15.1 ± 0.057
8	PrecirolATO5	Oleicacid	30:70	Tween 80 2%	238.8±2.136	0.645±0.01	-14.6 ± 0.2

particle size distribution in these formulae, more sonication time optimization may be required.

A small particle size is an advantage for VLP-NLC because it decreases uptake by the liver, prolongs circulation time in the blood, and improves bioavailability. Small particles are also minimally phagocytosed by macrophages, so destruction and clearance by the body is minimized (34, 35).

2-Measurement of the surface charge of VLP-NLCs

For full electrostatic stabilization, the zeta potential must be greater than +30 mV or less than −30 mV (36). A potential is created around the particle by its surface charge; it is greatest near the surface and gets smaller as it moves deeper into the medium. This potential, known as the zeta potential, is crucial to the stability of dispersions because it prevents particles from adhering together to form larger particles. All peppered VLP-NLCs had negative zeta potential. As shown in (Table 2), the eight produced NLCs' zeta potential values ranged from -14.6 ± 0.2 to - 46.0 ± 1.1 mV for different Formulae.

By creating a coat on their surface and reducing the electrostatic repulsion between the particles, surfactant can stabilize NLCs. In addition to the steric stabilization of nanoparticles caused by the use of Tween 80 as surfactant, it is evident that high zeta potential, close to -30 mV for the selected NLC 6, may due to the type of liquid lipid used.

Oleic acid usage increased the negative charge on molecules' surfaces to a high level. This may be the result of the presence of a strong carboxyl group with a significant negative charge in Oleic acid structure. According to previous studies, the selected NLC 6 zeta potential that equals -26 mV was found to be high enough to produce a stable colloidal nanosuspension (37).

3- Determination of EE% of VLP in NLC formulae

From the data listed in (Table 3), the highest encapsulation efficiency value of VLP was found to be for NLC 6 with 89.1 % ± 3.3, while the lowest value was in formula NLC 7 by 79.8 % ± 2.5.

The high EE of VLP in the NLCs could be attributed to the presence of the liquid nano-compartment formed by oleic acid, which were trapped within the solid NLCs matrix. Therefore, NLCs acted as VLP drug delivery devices in nano reservoirs. Comparable results have achieved previously (38).

They discovered that freshly made NLCs of docetaxel have EE equals to 89.1 % on average. While Tiwari and Pathak have mentioned that the EE of nanoparticles was increased from 81.74% to 93.33% respectively upon increasing the percentage ofoleic acid from 15 to 30 weight percent (39).

Table 3. Encapsulation efficiency of VLP-NLCs

Formula	**1**	**2**	**3**	**4**	**5**	**6**	**7**	**8**
EE%	88.8% ±0.14	87.6 % ±2.7	86.30% ±0.21	84.07% ±0.92	82.9% ±3.6	89.1% ±3.3	79.8% ±2.5	83.6% ±0.7

4-Differential Scanning Calorimetry Analysis

Generally, the melting points of a colloidal system may decrease by 10°C–15°C, because colloidal particles have a large surface to volume ratio. The apparent reduction in melting point of colloid formulations is not associated with particle size (40).

A DSC study offers a thorough examination of the behavior of crystalline materials, such as lipid nanoparticles, during melting and crystallization. The major objective of this investigation was to determine whether the composition of each formula caused any differences in the lipid matrix.

An endothermic peak of VLP was found at 75° C. as mentioned in previous study (41). The endothermic peak of Precirol ATO 5 appeared at 64 ° C (42) (Fig. 3). The physical mixtures showed the endothermic peak of the lipid and the drug with no shift indicating that both of them were in the crystalline form in the binary mixture in the ratio (1:1).

For amorphous solids or less ordered crystals, the melting of the substance consumes much less energy than crystalline substances which need to overcome lattice forces (43).

From previous obtained results, it has been concluded that the lipid in the nanoparticles should be in a less ordered arrangement compared to the bulk lipid. The addition of the liquid lipid to the nanoparticles decreases the crystallinity of the lipid matrix. A less ordered crystal or amorphous lipid matrix would be favorable for encapsulating more drug molecules thus enhancing DL and prolonging the drug release of the lipophilic drug from the lipid matrix.

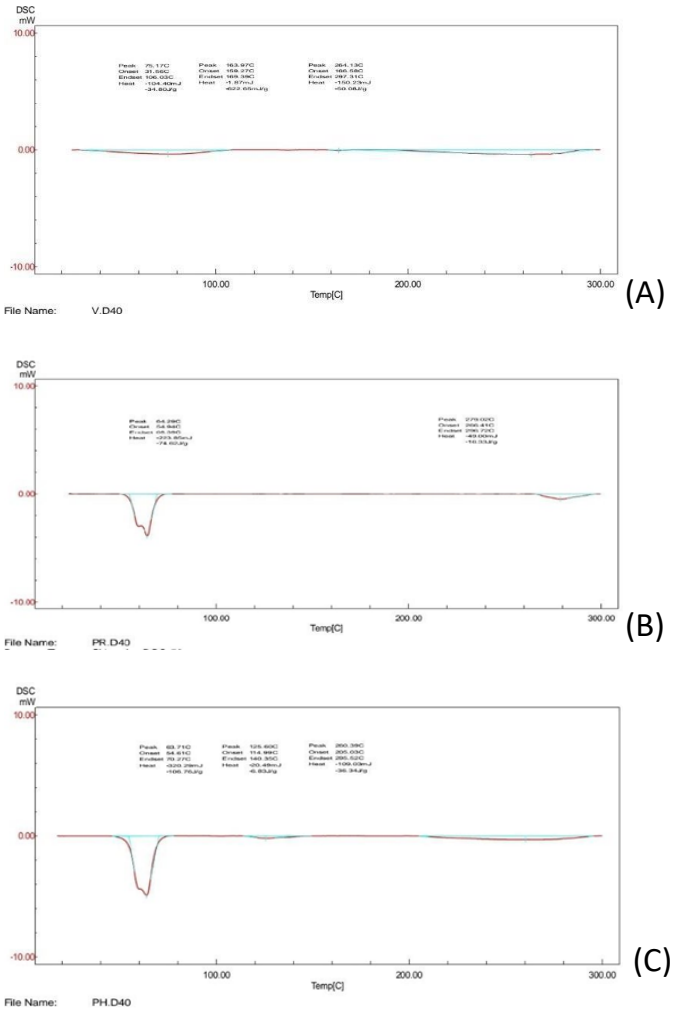

Figure 3. DSC thermograms of (A) VLP, (B) Precirol ATO 5 and (C) physical mixture

5-Transmission electron microscopy examination (TEM)

The TEM photographs of the selected NLC6 formula are shown in (**Fig. 4**) in which lipid nanoparticles were magnified by two different magnifications (48000, 72000 times). From these figures, it is obvious that nanoparticles in the formulation are mainly discrete entities. All particles were in the nanometer range. The TEM analysis also showed that the NLC6 nanoparticles were uniform in size and shape, either spherical or elliptical. This demonstrates high uniformity and homogeneity that may lead to the entrapped VLP being released uniformly. TEM assessmentof particles may result in reduced particle size due to the drying of the sample (44, 45).

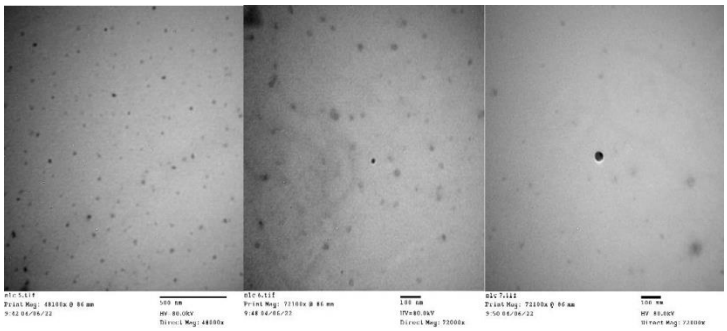

Figure 4. TEM photographs of the selected NLC formula (NLC 6) by different magnifications X48000, X72000.

6-Wide angle X-ray diffraction (XRD)

Wide angle X-ray diffraction is an analytical tool complementary to differential scanning calorimetry in the assessment of degree of crystallinity and polymorphism of a bulk solid lipid, drug, and 1:1 of their physical mixture. Thus, the wide-angle X-ray diffractogram parallels the results obtained by differential scanning calorimetric thermal analysis.

The X-ray diffraction patterns for Precirol ATO5, pure VLP, and VLP: Precirol 1:1 physical mixture is shown in (Fig.5), and indicates that VLP produced a diffraction pattern with multiple peaks. A relatively sharp peak was observed for Precirol ATO 5 one characteristic peak appeared at 20 2θ (42). The diffraction peaks for physical mixture were found to be broader, less intense and more diffused than that of pure VLP and Precirol ATO5.

7- Fourier transform-infrared spectroscopy

The FTIR spectroscopy is done on pure VLP powder and Precirol and 1:1 binary physical mixture of the drug and the solid lipid to investigate possible incompatibilities may occur. As shown in (**Fig. 6**) the FTIR spectra of VLP, Precirol ATO 5 and a binary mixture of equal ratios of both ingredients respectively.

VLP spectrum shows different characteristic vibrational peaks of VLP. Broad peakat 3485 and 3439 cm^{-1} respectively are specific for (N–H) and (O–H) stretching. Peaks in the range of 2873 and 2963 cm^{-1} are characteristic peaks for CH3 (–C–H) stretching. It also had characteristic peak at 1637 cm^{-1} which is corresponding to carbonyl group (C = O) (41).

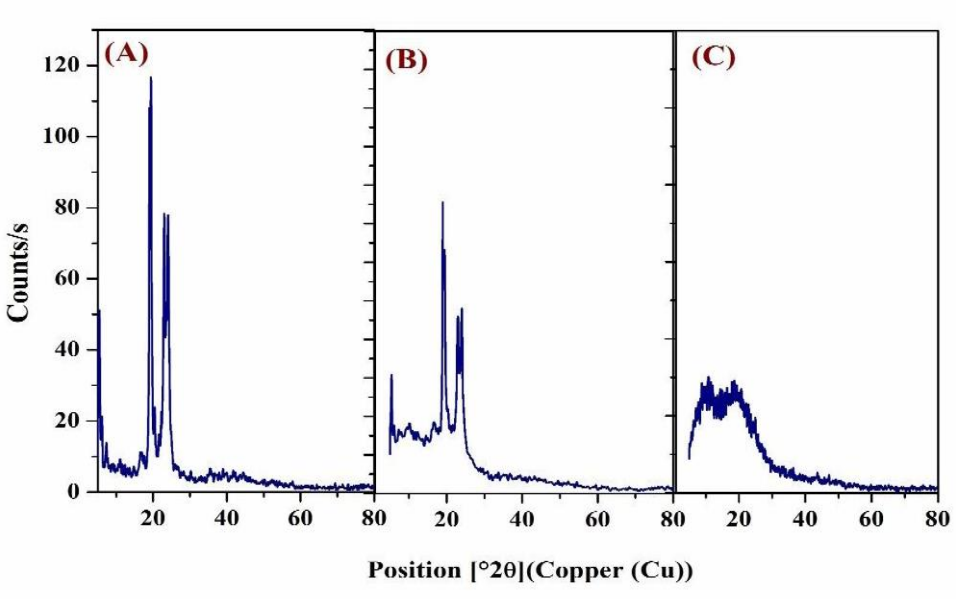

Figure 5. XRD pattern of (A) Precirol ATO 5, (B) 1:1 Physical mix. and (C) VLP

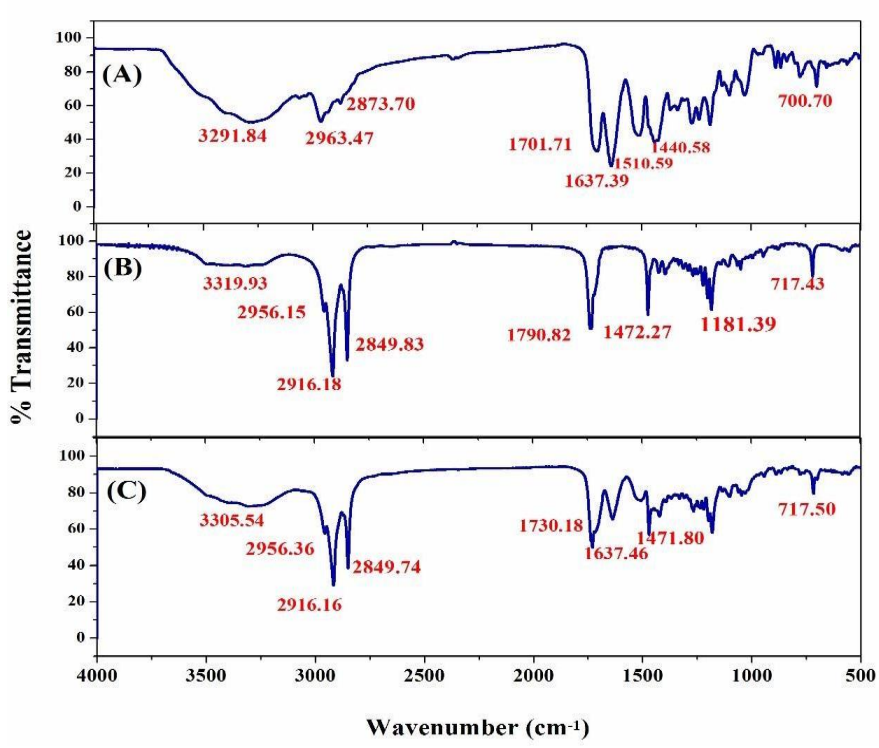

Figure 6. (FT IR) spectra of (A) VLP, (B) Precirol ATO5, (C) 1:1 physical mixture

According to the chemical structure of Precirol ATO 5, it presents the following characteristic bands: major peak at 1730 cm^{-1} due to (C=O) stretching and 2916cm−1 of (C-H) stretching, which are characteristic of Precirol ATO 5 (46). In the binary mixture spectrum, a combination of characteristic peaks for the functional groups in both substances is observed. Peaks corresponding to the carbonyl group, CH3 and C–H stretching appeared in the same wave number rangeas the pure VLP powder. This indicates that both drug and lipid remained unchanged.

8-In Vitro Release of VLP-NLCs

The In Vitro release profile was evaluated by dialysis for 24 hours at predetermined time intervals. (Fig. 7 and 8) show the release profile of selected VLP NLC 6 formula compared to that of pure VLP in buffer PH 1.2 and 6.8 respectively. NLC 6 showed consistently, time- dependent and prolonged VLP release.

The release mechanism might be explained by the fact that the solid lipid core of the nanoparticles was spread throughout with liquid lipids at the outside shell. This allowed the liquid lipid-enriched outer layers to load more medicine that could be released more readily. Hence, the nanoparticles displayed rapid release at the first stage. Then, the medication integrated into the solid-lipid core was released in a sustained pattern due to erosion or degradation of lipid matrix (47).

The difference between the release properties of pure VLP and VLP-NLCs is evidently attributed to the prolonged release function of NLC. Lipophilic poorly water soluble VLP was held by the lipid core of the NLC and the drug released mainly through dissolution and diffusion. This result implied that VLP could be

released slowly from VLP-NLCs and could keep constant concentration for relatively longer period.

In drug release medium of pH 6.8, NLCs boost the dissolution profile of VLP as shown in Figure 8. By reduction of the drug particle size to nanometer range and suppression the crystallization of VLP, NLCs make the VLP more soluble and overcome the pH-dependent bioavailability issues related with oral administration of VLP.

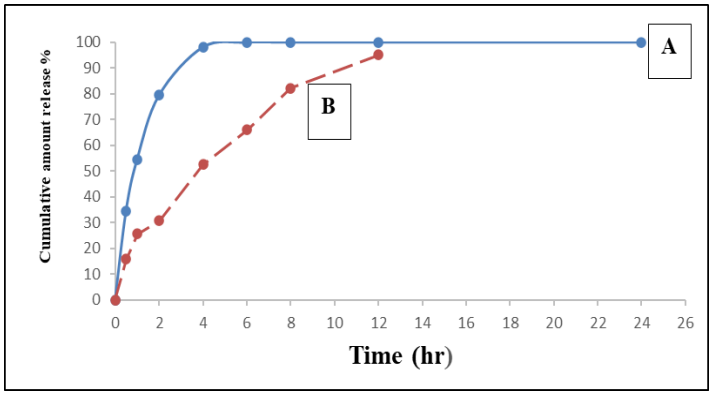

Figure 7. Release profiles of (A) VLP and (B) NLC 6 in buffer (pH 1.2)

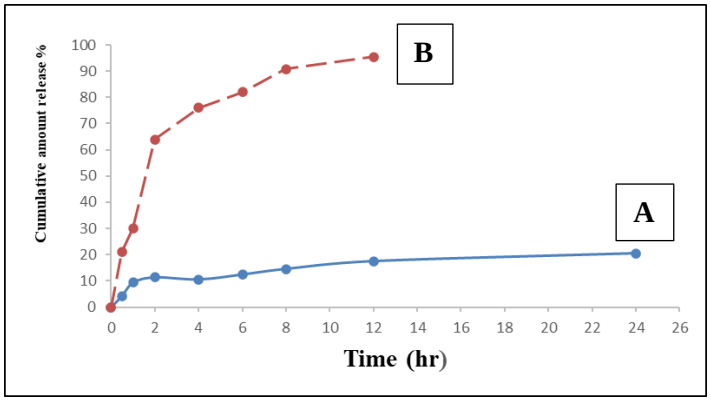

Figure 8. Release profiles of (A) VLP and (B) NLC 6 in buffer (pH 6.8)

Conclusion

VLP was successfully incorporated into NLC using the homogenization- ultrasonication technique. Using Precirol ATO5 as solid lipid and oleic acid as a liquid lipid resulted in a decrease in particle size and increase in EE. VLP incorporated into NLC was in amorphous form as confirmed by DSC analysis. NLC 6 had the best overall rank compared to all prepared formulae. Formulation of VLP in NLC enhanced its efficacy hence its oral dose can be lowered.

References

[1] Gao L, Zhang D, M. C. Drug nanocrystals for the formulation of poorly soluble drugs and its application as a potential drug delivery system. J Nanopart Res. 2008; 10: 845-62.
[2] Seenivasan A., Panda T. Lovastatin nanoparticle synthesis and characterization for better drug delivery. Open Biotechnol J. 2011; 5: 28-32.
[3] Souto E.B., Wissing S.A., Barbosa C.M., R.H. M. Development of a controlled release formulation based on SLN and NLC for topical clotrimazole delivery. Int J Pharm. 2004; 278: 71-7.
[4] Abbasalipourkabir R., Salehzada A., A. R. Solid lipid nanoparticles as new drug delivery system. Indian J Pharm Sci. 2011; 2: 252-61.
[5] Junghanns J.H., R.H. M. Nanocrystal technology, drug delivery and clinical applications. Int J Nanomedicine. 2008; 3: 295.
[6] Patidar A., Thakur D.S., Kumar P., J. V. A review on novel lipid based nanocarriers. Int J Pharmacol Pharm Sci. 2010; 4: 30-5.
[7] Ioana L., Nicoleta B., Alina M., M. A. The encapsulation effect of UV molecular absorbers into biocompatible lipid nanoparticles. Nanoscale Res Lett. 2011; 6: 73-82.
[8] Mistry S.N, Patel P.K., Bharadia P.D., Pandya V.M., D.A. M. Novel drug delivery system for lipophilic agents: solid lipid nanoparticles. J Pharm Cosmetol. 2011; 1: 76-89.
[9] Shaji J., V. J. Solid lipid nanoparticles: a novel carrier for chemotherapy. Int J Pharmacol Pharm Sci. 2010; 2: 8-17.
[10] Pardeike .J, Hommoss A., R.H. M. Lipid nanoparticles (SLN, NLC) in cosmetic and pharmaceutical dermal products. Int J Pharm. 2009; 366: 170-84.
[11] Müller R.H., Mäder K., S. G. Solid lipid nanoparticles (SLN) for controlled drug delivery - a review of the state of the art. Eur J Pharm Biopharm. 2000; 50: 161-77.
[12] Bhatt D., Pethe A. Lipid technology - a promising drug delivery system for poorly water soluble drugs. Int. J. Pharm. Res. Dev. 2010; 2.
[13] G.A. H. Nanostructure-mediated drug delivery. Nanomedicine. 2005; 1: 22-30.
[14] Müller R.H., Radtke M. Solid lipid nanoparticles (SLN) and nanostructured lipid carriers (NLC) in cosmetic and dermatological preparations. Adv Drug Deliv Rev. 2002; 54: S131–S55.
[15] Müller R.H., Radtke M., S.A. W. Nanostructured lipid matrices for improved microencapsulation of drugs. Int J Pharm. 2002; 242: 121-8.
[16] Mehanna M., Motawaa A., M. S. Pharmaceutical particulate carriers: lipid-based carriers. Natl J Physiol Pharm Pharmacol. 2012; 2: 10-22.
[17] Gregory J. D., B. S. Hepatitis C virus elimination: laying the foundation for achieving 2030 targets. Nat. Rev. 2021; 18: 91-2.
[18] Dore G. J., J. FJ. Hepatitis C virus therapeutic development: in pursuit of "perfectovir". Clin Infect Dis. 2015; 60: 1829-36.
[19] Mrinalini C. D., K. PB. Stability Indicating HPTLC Method for Sofosbuvir and Velpatasvir in Combination. Int. J. Pharm Sci Drug. Res. 2020; 12: 129-35.
[20] Reema M., Dhara P., Khushboo P., M. D. Development And Validation Of Three Novel UV Spectrophotometric Methods For Determination Of Newly Discovered Combination For The Treatment Of Hepatitis C And Their Comparison Using ANOVA. Int J Pharm Drug Anal. 2018; 6(3): 391-9.
[21] Cory T.J., Mu Y., Gong Y. KS, S. K. Sofosbuvir+ velpatasvir+ voxilaprevir for the treatment of hepatitis C infection. Expert Opin Pharmacother. 2018; 19: 749–57.
[22] Dahan A., Miller J.M., G.L. A. Prediction of solubility and permeability class membership: Provisional BCS classification of the world's top oral drugs. AAPS J. 2009; 11: 740–6.
[23] Kong F., R.P. S. Disintegration of solid foods in human stomach. J Food Sci. 2008; 73: R67–R80.
[24] Karamanolis G., Theofanidou I., Yiasemidou M., Giannoulis E., Triantafyllou K., S.D. L. A Glass of Water Immediately Increases Gastric pH in Healthy Subjects. Dig Dis Sci. 2008; 53: 3128–32.
[25] Nair H.B., Sung B., Yadav V.R., Kannappan R., Chaturvedi M.M., B.B. A. Delivery of antiinflammatory nutraceuticals by nanoparticles for the prevention and treatment of cancer. Biochem. Pharmacol. 2010; 80: 1833-43.
[26] Riehemann K., Schneider S.W., Luger T.A., Godin B., Ferrari M., H. F. Nanomedicine challenge and perspectives. Angew. Chem. 2009; 48: 872-97.
[27] Das S., A. C. Recent advances in lipid nanoparticle formulations with solid matrix for oral drug delivery. AAPS PharmSciTech. 2011; 12: 62-76.
[28] Dubey A., Prabhu P., J.V. K. Nano Structured lipid carriers : A Novel Topical drug delivery system. Int. J. Pharmtech Res. 2012; 4: 705-14.
[29] Orive G., Anitua E., Pedraz J.L., D.F. E. Biomaterials for promoting brain protection, repair and regeneration. Nat. Rev. Neurosci. 2009; 10: 682-92.
[30] Peer D., R. M. Fluoxetine and reversal of multidrug resistance. Cancer Lett. 2006; 237: 180-7.
[31] Huang Q., Yu H., Q. R. Bioavailability and delivery of nutraceuticals using nanotechnology. J. Food Sci. 2010; 75: 50-7.
[32] Eid E.M., Abdul A.B., Suliman F.E., Sukari M.A., Rasedee A., S.M. F. Characterization of the inclusion complex of zerumbone with hydroxypropyl-β-cyclodextrin. Carbohydr Polym. 2011; 83: 1707-14.
[33] Zhang Y, Zhi Z, Jiang T, Zhang J, Wang Z, Wang S. Spherical mesoporous silica nanoparticles for loading and release of the poorly water-soluble drug telmisartan. JCR. 2010; 145: 257-63.
[34] Fang Y.P., Lin Y.K., Su Y.H., J.Y. F. Tryptanthrin-loaded nanoparticles for delivery into cultured human breast cancer cells, MCF7: the effects of solid lipid/liquid lipid ratios in the inner core. Chem Pharm Bull. 2011; 59: 266-71.
[35] De Jong W.H., JA. P. Drug delivery and nanoparticles: applications and hazards. Int J Nanomedicine. 2008; 3: 133-49.
[36] Thatipamula R.P., Palem C.R., Gannu R., Mudragada S., M.R. Y. Formulation and in vitro characterization of domperidone loaded solid lipid nanoparticles and nanostructured lipid carriers. DARU J. Pharm. Sci. 2011; 19: 23-32.
[37] Velmurugan R., S. S. Development and optimization of ifosfamide nanostructured lipid carriers for oral delivery using response surface methodology. Appl. Nanosci. 2015; 1-15.

[38] Liu D., Liu Z., Wang L., Zhang C., N. Z. Nanostructured lipid carriers as novel carrier for parenteral delivery of docetaxel. Colloids surf. B. 2011; 85: 262-9.
[39] Tiwari R., K. P. Nanostructured lipid carrier versus solid lipid nanoparticles of simvastatin: comparative analysis of characteristics, pharmacokinetics and tissue uptake. Int. J. Pharm. 2011; 415: 232-43.
[40] Wan F., You J., Sun Y., Xing G.Z., D.C. F. Studies on PEG-modified SLNs loading vinorelbine bitartrate (1): preparation and evaluation in vitro. Int. J. Pharm. Sci. 2008; 359: 104-10.
[41] Mehmood Y., Ullah Khan I., Shahzad Y., Ullah Khan R., Shahid Iqbal M., Ahmad Khan H., et al. In-Vitro and In-Vivo Evaluation of VelpatasvirLoaded Mesoporous Silica Scaffolds. A Prospective Carrier for Drug Bioavailability Enhancement. Pharmaceutics. 2020; 12.
[42] Patro N.M., Devi K., Pai R.S., S. S. Evaluation of bioavailability, efficacy, and safety profile of doxorubicin-loaded solid lipid nanoparticles. J Nanopart Res. 2013; 15.
[43] Hou D., Xie C., Huang K., C. Z. The production and characteristics of solid lipid nanoparticles (SLNs). Biomaterials. 2003; 24: 1781-5.
[44] Liu J., Gong T., Wang C., Zhong Z., Z. Z. Solid lipid nanoparticles loaded with insulin by sodium cholate-phosphatidylcholinebased mixed micelles: preparation and characterization. Int. J. Pharm. 2007; 340: 153-62.
[45] Sanad R.A., Abdelmalak N.S., Elbayoomy T.S., A.A. B. Formulation of a novel oxybenzone-loaded nanostructured lipid carriers (NLCs). AAPS PharmSciTech. 2010; 11(4): 1684-94.
[46] Youssef A., Dudhipala N., S. M. Ciprofloxacin Loaded Nanostructured Lipid Carriers Incorporated into In-Situ Gels to Improve Management of Bacterial Endophthalmitis. Pharmaceutics. 2020; 12.
[47] Jia L., Shen J., Zhang D., Duan C., Liu G., Zheng D., et al. In Vitro and in vivo evaluation of oridonin-loaded long circulating nanostructured lipid carriers. Int. j. biol. macromol. 2012; 50: 523-9.